Thermal Performance Evaluation of Attic Radiant Barrier Systems Using the Large Scale Climate Simulator (LSCS)

Som Shrestha, PhD
Member ASHRAE

William Miller, PhD
Member ASHRAE

Andre Desjarlais

ABSTRACT

Application of radiant barriers and low-emittance surface coatings in residential building attics can significantly reduce conditioning loads from heat flow through attic floors. The roofing industry has been developing and using various radiant barrier systems and low-emittance (low-e) surface coatings to increase energy efficiency in buildings; however, minimal data are available that quantify the effectiveness of these technologies.

This study evaluates performance of various attic radiant barrier systems under simulated summer daytime conditions and nighttime or low solar gain daytime winter conditions using the large scale climate simulator (LSCS). The four attic configurations that were evaluated are 1) no radiant barrier (control), 2) perforated low-e foil laminated oriented strand board (OSB) deck, 3) low-e foil stapled on rafters, and 4) liquid applied low-emittance coating on roof deck and rafters. All test attics used nominal R_{US} 13 h·ft^2·°F/Btu (R_{SI} 2.29 m^2·K/W) fiberglass batting insulation on the attic floor. Results indicate that the three systems with radiant barriers had heat flows through the attic floor during summer daytime condition that were 32.8%, 49.8%, and 19.1% lower than the control, respectively.

INTRODUCTION

Among the various modes of heat transfer, radiation is the predominant mode of heat transfer in typical building attics, particularly during summer months. Therefore, the use of radiant barriers or low-emittance (low-e) surface coatings in residential building attics can significantly reduce conditioning loads from heat flow through attic floors. In order to determine the effectiveness of various radiant barrier systems, the Building Envelope Research (BER) group within the Building Technologies Research and Integration Center (BTRIC) at Oak Ridge National Laboratory (ORNL) conducted a series of steady-state guarded hot box evaluations in the large scale climate simulator (LSCS) from May to August 2011. Results from this study are presented in this paper.

DESCRIPTION OF THE TEST APPARATUS

The large scale climate simulator (Figure 1) is a facility that is capable of testing whole roof and attic systems under either steady-state or transient conditions. The climate chamber of the LSCS can expose specimen to ambient temperatures ranging from –40°F (–40°C) to 150°F (65.6°C). The roof surface can be maintained at a higher temperature than the climate chamber air temperature because it can be heated with infrared lamps that can be controlled to simulate solar heat gain. The lower portion of the LSCS contains both a guard and a metering chamber, each of which can be controlled independently from 45°F (7.2°C) to 150°F (65.6°C). Both upper and lower chambers have controlled humidity and other capabilities that were not utilized in this set of experiments. Figure 2 shows the test attic in the LSCS environmental chamber.

The LSCS can be operated as an environmental chamber (heat flows through the ceiling are measured with heat flux transducers attached to it) or as a guarded horizontal hot box test facility. Guarded hot box tests are conducted in accordance with ASTM C1363-05 *Standard Test Method for Thermal Performance of Building Materials and Envelope*

***Som Shrestha**, **William Miller**, and **Andre Desjarlais** are affiliated with the Building Technologies Research and Integration Center, Oak Ridge National Laboratory, Oak Ridge, TN.*

Published by ASHRAE 2013

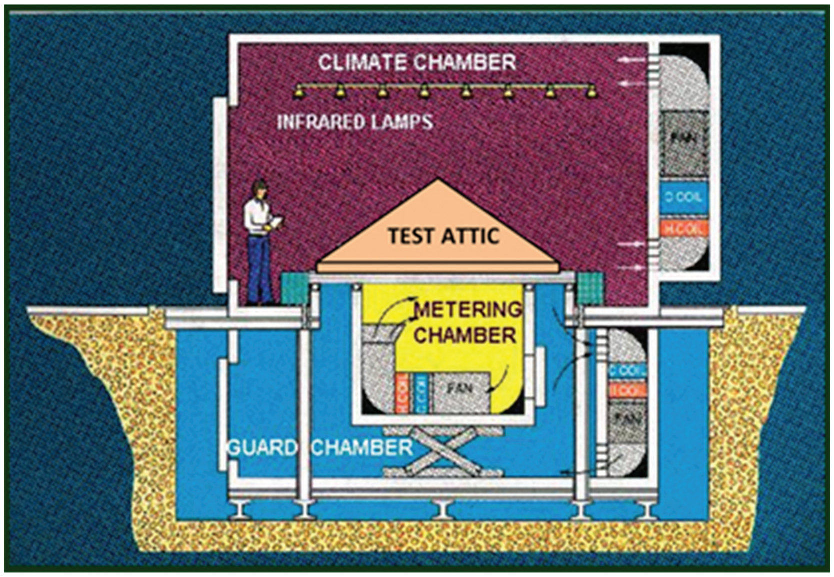

Figure 1 *Sketch of the large scale climate simulator (LSCS).*

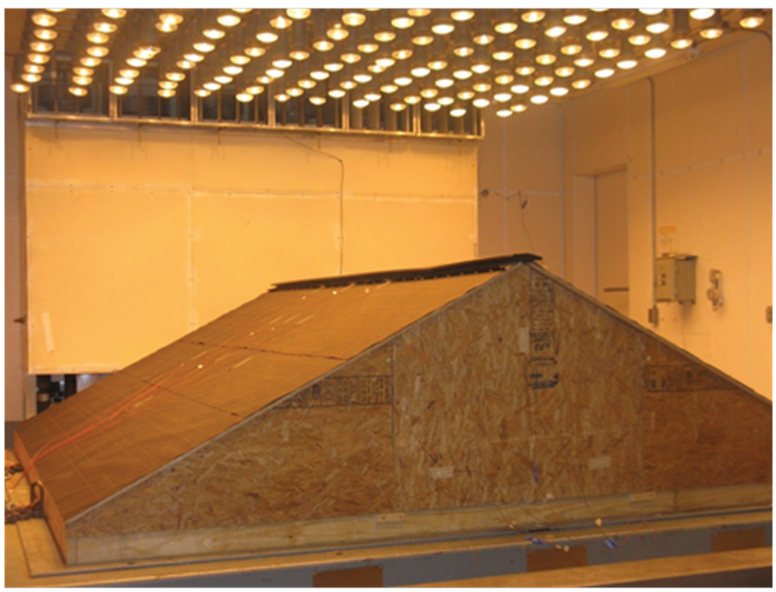

Figure 2 *The test attic in the LSCS environmental chamber.*

Assemblies by Means of a Hot Box Apparatus or in accordance with ASTM C1373-03 *Standard Practice for Determination of Thermal Resistance of Attic Insulation Systems Under Simulated Winter Conditions*. The chamber is designed to test the thermal performance of 12 ft, 9 in by 12 ft, 9 in (3.9 m by 3.9 m) roof sections and all controls and data acquisitions are automatic and programmable. Details of the LSCS are described by Huntley (1989).

The metering chamber serves as a guarded hot box. The chamber is manually raised so that it seals against the ceiling, and provides a measurement of the total heat flow through the 8 ft (2.44 m) by 8 ft (2.44 m) central area of the attic floor. The surrounding guard chamber temperature is maintained close to the metering chamber temperature to minimize heat flows across the metering chamber walls. Heat flow through the attic floor can then be calculated from an energy balance of the metering chamber (Wilkes et al., 1995). The tests described in this paper were conducted in this manner.

Prior to the test, the metering chamber was calibrated with a series of experiments conducted on a homogeneous panel made of 4 in. (0.102 m) of expanded polystyrene (EPS) foam (with known R-value) which was painted on both sides with white latex paint. The calculated bias from this calibration test was used to adjust the collected experimental data. The precision and bias test procedure for the LSCS is described by Wilkes et al. (1995).

DESCRIPTION OF THE TEST ATTIC

The test attic module was 12 ft, 8 in. (3.86 m) by 12 ft, 8 in. (3.86 m) with 6:12 roof slope (Figure 2). Nominal 2 by 4 (actual 1.5 in. [38 mm] by 3.5 in. [89 mm]) rafters and ceiling joists were spaced at 24 in. (0.61 m) on center. Nominal R_{US} 13 h·ft^2·°F/Btu (R_{SI} 2.29 m^2·K/W) fiberglass batting insulation was installed between the joists. The insulation was 3.5 in. (89 mm) thick; therefore, the top of the attic floor insulation was level with the top edge of the ceiling joists. A ½ in. (13 mm) gypsum board was used on the ceiling. The roof consisted of nominal ¾ in. (19 mm) oriented strand board (OSB) and 15 lb (6.8 kg) roofing felt. Ridge vents and eaves made by drilling holes were used to achieve a net free ventilation area of 1:150 (total unobstructed cross-sectional area of ventilation openings of 1 ft^2 for every 150 ft^2 [0.093 m^2 for every 13.94 m^2] of attic floor area).

The performance of the following four attic configurations was evaluated:

Attic 1: ordinary OSB without radiant barrier (control)

Attic 2: perforated low-e foil laminated on OSB (TechShield) (Figure 3)

Attic 3: low-e foil stapled on rafters (Figure 4)

Attic 4: liquid applied low-e coating on roof deck and rafters (Figure 5)

The thermal emittance of the OSB, radiant barrier materials, and the OSB with low-e coating were measured using Devices & Services emissometer model AE which was operated in accordance with ASTM C1371 *Standard Test Method for Determination of Emittance of Materials Near Room Temperature Using Portable Emissometers* or Devices and Services Technical Note 79-17 (transient method). Table 1 shows the measured emittances. The foil stapled on rafters had a low-e surface on both sides. The specimen with liquid applied low-e on OSB was cured at 410°F (210°C) for about 30 minutes prior to measuring the thermal emittance.

Figure 3 *Test attic with low-e foil laminated on OSB.*

Table 1. Measured Thermal Emittance of Materials

Material	Measured Average Thermal Emittance, ε	Measurement Method
OSB	0.89	Transient
Perforated low-e foil laminated on OSB	0.03	Transient
Low-e foil stapled on rafters	0.02	ASTM C1371
Low-e coated on OSB	0.23	Transient
Rafters	0.87	Transient

Figure 4 *Test attic with low-e foil stapled on rafters.*

Figure 5 *Test attic with liquid applied low-e coating on roof deck and rafters.*

TEST DESCRIPTION

The tests were conducted in laboratory environments simulating summer daytime and winter nighttime or low solar gain daytime conditions for a cooling dominant climate zone. For the summer daytime condition, the climate chamber air temperature around and above the test attic was set to 100°F (37.8°C) and the IR lamps were used to maintain roof exterior surface temperature at 140°F (60.0°C). For the winter night condition, the climate chamber air temperature was set to 32°F (0°C) and the infrared lights were turned off (the roof exterior surface temperature was not controlled). These conditions were selected based on AtticSim (attic simulation software developed at ORNL, Wilkes 1991) simulation result using TMY3 weather file for Austin, TX. Metering chamber temperature (measured at about 3 in. (76 mm) below the attic floor) and the guard chamber temperatures were set at 70°F (21.1°C) in both cases to simulated indoor conditions.

In total; 5 thermocouples were used to measure the climate chamber air temperature, 20 thermocouples were used to measure the roof exterior surface temperature, 13 thermocouples were used at various heights to measure the attic air temperature, 5 thermocouples were used to measure the attic floor temperature on top of the insulation, and 5 thermocouples were used to measure the temperature of the gypsum board surface facing the metering chamber. Averages of the measured temperatures are presented in Table 2. As can be seen from the table, the climate chamber air temperature was maintained within ± 0.5°F (± 0.3°C) of the setpoint tempera-

Table 2. Average of the Measured Temperatures

Measurement Location	Attic Configuration	Summer Day Condition	Winter Night Condition
Climate Chamber Air Temperature, °F (°C)	Attic 1	99.8 (37.7)	32.0 (0.0)
	Attic 2	100.1 (37.8)	31.9 (–0.1)
	Attic 3	99.5 (37.5)	32.1 (0.1)
	Attic 4	99.9 (37.7)	32.1 (0.0)
Roof Exterior Surface Temperature, °F (°C)	Attic 1	140.5 (60.3)	32.2 (0.1)
	Attic 2	140.6 (60.3)	32.0 (0.0)
	Attic 3	139.6 (59.8)	32.2 (0.1)
	Attic 4	139.5 (59.7)	32.0 (0.0)
Attic Air Temperature, °F (°C)	Attic 1	120.2 (49.0)	33.9 (1.1)
	Attic 2	111.1 (44.0)	35.0 (1.7)
	Attic 3	105.6 (40.9)	38.5 (3.6)
	Attic 4	114.1 (45.6)	34.6 (1.4)
Attic Floor Temperature, °F (°C)	Attic 1	121.3 (49.6)	37.1 (2.8)
	Attic 2	105.7 (40.9)	39.2 (4.0)
	Attic 3	98.1 (36.7)	41.9 (5.5)
	Attic 4	110.7 (43.7)	38.3 (3.5)
Gypsum Board Surface Temperature Towards the Metering Chamber, °F (°C)	Attic 1	74.6 (23.7)	68.1 (20.0)
	Attic 2	73.2 (22.9)	68.2 (20.1)
	Attic 3	72.6 (22.6)	68.4 (20.2)
	Attic 4	73.7 (23.2)	68.2 (20.1)
Metering Chamber Air Temperature, °F (°C)	Attic 1	70.0 (21.1)	69.9 (21.1)
	Attic 2	70.0 (21.1)	70.0 (21.1)
	Attic 3	70.1 (21.1)	70.0 (21.1)
	Attic 4	70.0 (21.1)	70.0 (21.1)
Gable Exterior Surface Temperature, °F (°C)	Attic 1	105.0 (40.5)	32.8 (0.4)
	Attic 2	102.1 (38.9)	32.6 (0.3)
	Attic 3	100.8 (38.2)	33.9 (1.0)
	Attic 4	102.6 (39.2)	32.8 (0.4)

ture, the roof exterior surface temperature was maintained within ± 0.6°F (± 0.33°C) of the setpoint temperature, and the metering chamber air temperature was maintained within ±0.1°F (± 0.06°C) of the setpoint temperature.

RESULTS AND DISCUSSION

The rate of heat flow to or from the metering chamber through the attic floor was calculated by conducting an energy balance calculation in the metering chamber. The rate of heat flow was converted to heat flux by dividing the effective area of the ceiling exposed to the metering chamber, which is 64 ft^2 (5.95 m^2).

Energy in and out of the metering chamber, including the heat flow through the metering chamber walls due to the negligibly small imbalance between the metering and guard chamber air temperatures, was measured in accordance with ASTM C1363. After the steady-state conditions were reached, data from each sensor were recorded for 18 hours at 5 minute intervals. Time constant of the LSCS is approximately 3 hours; therefore, 18 hours period is equivalent to six time-constants of the LSCS. Energy balance calculations on the metering chamber were performed for each five-minute interval, and these values were averaged over the 18-hour period to calculate an average heat flow through the attic floor. Heat flows through the metering chamber walls were estimated using 32 differential thermocouples across the walls.

Figure 6 shows the hourly cooling load during summer daytime condition and heating load during winter condition to the metering chamber due to the heat flow through the attic floor. The error bars on the plot show the two standard deviations of the calculated average hourly values over the same period. The calculated heating and cooling loads, heat flux, and 95% reproducibility intervals are shown in Table 3.

The key measure of the thermal performance of the radiant barrier is the percentage reduction in heat flow to conditioned space caused by the use of the radiant barrier. From Table 3, it can be seen that the test attic with perforated low-e foil laminated OSB deck, low-e foil stapled on rafters, and liquid applied low-e coating reduced the cooling load from the attic floor compared to the load from the attic without a radiant barrier on roof deck by 32.8% ± 4.9%, 49.8% ± 3.2%, and 19.1% ± 3.7%, respectively, during summer daytime conditions and by 8%, 10%, and 6%, respectively, during winter conditions. However, while the result is statistically significant with better than 95% confidence for summer condition, the result is not statistically significant at the same level for winter condition.

It should be noted that the attic with low-e foil stapled on rafters had 3.5 in. (88.9 mm)-high air space between the foil and roof sheathing. Air movement in these cavities takes away some of the heat penetrated through roof sheathings (similar to the case with above-sheathing ventilation design, as described in Miller et al. 2007), reducing heat flow to attic.

It should also be noted that, due to the limitations in the LSCS capability to control radiation heat flux from infrared light source, the exterior roof surface temperature was held fixed in all attic configurations for a given climate condition. If these tests were conducted in an actual building exposed to natural conditions, the exterior roof surface temperatures would not be the same for all attics. It is expected that for similar environmental conditions, attic construction, and all other building parameters; the exterior roof surface temperature would be higher in an attic with low-e foil laminated on OSB or liquid applied low-e coating on roof deck than in an attic without radiant barrier. The natural convection currents in attics with low-e foil stapled on rafters could feasibly drop the exterior roof surface temperature as compared to the case with foil faced OSB or liquid applied low-e coating on roof deck.

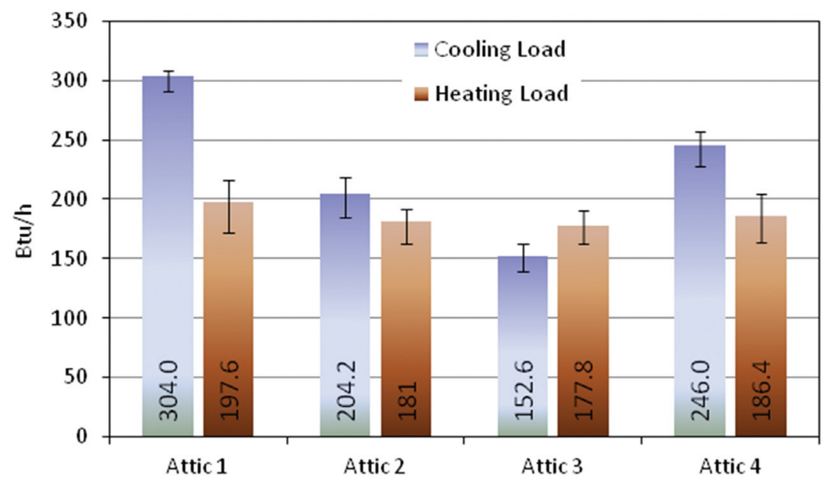

Figure 6 *Load to the metering chamber due to the heat flow through the attic floor.*

Table 3. Heating and Cooling Loads, 95% Reproducibility Intervals, and Heat Flux

Attic	Cooling Load		Heating Load		95% Reproducibility Intervals		Heat Flux, Summer		Heat Flux, Winter	
	Btu/h	W	Btu/h	W	Cooling Load, Btu/h (W)	Heating Load, Btu/h (W)	Btu/h·ft^2	W/m^2	Btu/h·ft^2	W/m^2
1 (Control)	304.0	89.0	197.6	57.9	± 4.4 (1.3)	± 18.2 (5.3)	4.8	15.0	–3.1	–9.7
2 (TechShield)	204.2	59.8	181.0	53.0	± 14.8 (4.3)	± 10.9 (3.2)	3.2	10.1	–2.8	–8.9
3 (Foil Stapled on Rafters)	152.6	44.7	177.8	52.1	± 9.4 (2.8)	± 12.4 (3.6)	2.4	7.5	–2.8	–8.8
4 (Liquid Applied)	246.0	72.1	186.4	54.6	± 10.6 (4.3)	± 17.8 (5.2)	3.8	12.1	–2.9	–9.2

SUMMARY

Implementation of radiant barriers is becoming more prominent in building codes, like California's Title 24. The US Department of Energy (DOE) conducted elaborate tests for radiant barrier in attics at the large scale climate simulator at Oak Ridge National Laboratory. The purpose of this testing was to evaluate the performance differences in new construction and retrofit applications, as well as the performance differences between the radiant barrier sheet and the radiant barrier paint, also known as an interior radiant control coating (IRCC).

Results show that the use of perforated low-e foil laminated OSB deck, low-e foil stapled on rafters, and liquid applied low-e coating resulted in a decrease in heat flow to the conditioned space by 32.8% ± 4.9%, 49.8% ± 3.2%, and 19.1% ± 3.7%, respectively, when compared to the load from attic without a radiant barrier during laboratory conditions representative of summer daytime temperatures and irradiance. During winter conditions, a 6% to 10% reduction in heat loss through the ceiling was observed, but the results were not statistically significant at 95% confidence. The test attic had nominal R_{US} 13 h·ft^2·°F/Btu (R_{SI} 2.29 m^2·K/W) fiberglass batting insulation on the floor. The heat flow through the attic floor decreases with higher insulation R-values or during milder weather conditions. Therefore, for attics with higher insulation R-values the potential savings due to the application of radiant barrier systems will be lower than the results shown in this study.

The DOE was hopeful that the IRCC would offer better performance since spraying on IRCC paint is easier than installing a sheet radiant barrier once the house is built, but the IRCCs on the market today do not perform as well as a sheet radiant barrier.

In new construction, the radiant barrier laminated to the OSB sheathing is certainly the easiest and least expensive to install, but going to the added labor in installing a radiant barrier under rafters can result in greater savings. This may be for a variety of reasons, like the higher emissivity of the OSB, a lack of space between the barrier and the sheathing to vent, and the presence of the rafters below the barrier to reduce the coverage of the low emittance surface.

The most efficient method was the radiant barrier stapled on rafters. This particular experiment did not have HVAC ducts in the attic; homes with attic ducts could see even greater savings in the summer. Radiant barrier stapled on the rafters is the preferred method of installing a retrofit radiant barrier by the US DOE, ENERGY STAR®, California Title 24, ASTM International, RIMA International, and others.

FUTURE WORK

The experimental data can be used to calibrate an attic model developed in any building energy simulation software. The calibrated model then can be used to run an annual simulation with local weather data and calculate annual energy savings potential of the various radiant barrier systems and attic insulation level for various climate zones.

For this study, the exterior roof surface temperature was held fixed in all attic configurations for a given climate condition, which would not be exactly the same if the test was conducted at natural environmental condition. Therefore, further experimental study should be carried out in natural exposure buildings.

ACKNOWLEDGMENTS

This work was supported by the Building Technologies Program, U.S. Department of Energy. The author would like to acknowledge the contributions of Jerald Atchley who supervised the operation of the LSCS; R&D Services, who constructed the attic modules; and industry supporters, who provided materials to build the attic.

REFERENCES

ASTM C1363. 2005. *Standard Test Method for Thermal Performance of Building Materials and Envelope Assemblies by Means of a Hot Box Apparatus*, American Society of Testing and Materials, West Conshohocken, PA, 2005.

ASTM C1371. 2010. *Standard Test Method for Determination of Emittance of Materials Near Room Temperature Using Portable Emissometers*, American Society of Testing and Materials, West Conshohocken, PA, 2005.

ASTM C1373. 2003. *Standard Practice for Determination of Thermal Resistance of Attic Insulation Systems Under Simulated Winter Conditions*, American Society of Testing and Materials, West Conshohocken, PA, 2005.

Devices and Services Technical Note 79-17 Emissivity Measurements for In-Place Surfaces and for Materials with Low Thermal Conductivity http://www.devicesandservices.com/TechNotes/TN79-17.pdf

Miller, W., M. Keyhani, T. Stovall, and A. Youngquist. 2007. Natural Convection Heat Transfer in Roofs with Above

Sheathing Ventilation. Proceedings of the Thermal Performance of the Exterior Envelopes of Buildings X. December 2–7, 2007 Clearwater, Florida.

Huntley, W. R. 1989. Design Description of the Large Scale Climate Simulator, ORNL/TM-10675, Oak Ridge National Laboratory, Oak Ridge, TN, 1989.

Wilkes, K.E., and P.W. Childs. 1993. Thermal Performance of Clean Horizontal Radiant Barriers under Winter Conditions – Laboratory Measurements and Mathematical Modeling. *ASHRAE Transactions* 1993, Vol. 99, Pt. 1.

Wilkes, K.E., T.W. Petrie and P.W. Childs. 1995. Precision and Bias of the Large Scale Climate Simulator in the Guarded Hot Box and Cold Box Modes. Proceedings of the 21st International Thermal Conductivity Conference. Oak Ridge National Laboratory, Oak Ridge, TN.

Wilkes, K. E. 1991. *Thermal Model of Attic Systems with Radiant Barriers*. ORNL/CON-262. Oak Ridge, TN: Oak Ridge National Laboratory.